

Review

Biomechanics of temporo-parietal skull fracture

Narayan Yoganandan *, Frank A. Pintar

Department of Neurosurgery, Medical College of Wisconsin, 9200 West Wisconsin Avenue, Milwaukee, WI 53226, USA

Received 16 December 2003; accepted 16 December 2003

Abstract

This paper presents an analysis of research on the biomechanics of head injury with an emphasis on the tolerance of the skull to lateral impacts. The anatomy of this region of the skull is briefly described from a biomechanical perspective. Human cadaver investigations using unembalmed and embalmed and intact and isolated specimens subjected to static and various types of dynamic loading (e.g., drop, impactor) are described. Fracture tolerances in the form of biomechanical variables such as peak force, peak acceleration, and head injury criteria are used in the presentation. Lateral impact data are compared, where possible, with other regions of the cranial vault (e.g., frontal and occipital bones) to provide a perspective on relative variations between different anatomic regions of the human skull. The importance of using appropriate instrumentation to derive injury metrics is underscored to guide future experiments.

Relevance

A unique advantage of human cadaver tests is the ability to obtain fundamental data for delineating the biomechanics of the structure and establishing tolerance limits. Force–deflection curves and acceleration time histories are used to derive secondary variables such as head injury criteria. These parameters have direct application in safety engineering, for example, in designing vehicular interiors for occupant protection. Differences in regional biomechanical tolerances of the human head have implications in clinical and biomechanical applications.

Published by Elsevier Ltd.

Keywords: Experimental studies; Fracture tolerance; Human skull; Temporo-parietal region

1. Introduction

The skull bone and brain tissue are the principal contents of the human head. Housing the brain, the skull bone protects the soft tissue from deformations secondary to external forces. Mechanically-induced trauma, particularly impact forces, are routinely delivered to the complex anatomy of the skull in different ways. For example, falls often result in vertex impacts to the skull. Pediatric fall injuries generally belong to this type because of the increased weight of the pediatric head compared to the adult wherein the weight of the head is approximately 6% of body weight (Snyder, 1977). In contrast, in lateral motor vehicle impacts, because of the proximity of the impact vector to the head, contacts involve the side (temporo-parietal region)

of the human head (Gennarelli et al., 2002). The bony anatomy of the head is complex and three-dimensional (Agur and Lee, 1991). A significant majority of studies determining human tolerance to impact has focused on the frontal bone because frontal crashes received principal attention during the early years of biomechanical research; the currently adopted worldwide Standards to assess head injury use biomechanical criteria based on frontal impacts to human cadavers (McElhaney et al., 1976; Sances et al., 1986; Sances and Yoganandan, 1986; Sances et al., 1981; Yoganandan et al., 1998). For example, helmet standards (Snell, ANSI, and others) use peak acceleration at the center of gravity of a dummy head as the measure of head injury. Frontal impacts use a criterion derived from the integration of the resultant linear accelerations at the center of gravity of the head as a measure of injury (NHTSA, 2002). The applicability of these indices to temporo-parietal impacts is not proven (Gennarelli et al., 2002).

* Corresponding author.

E-mail address: yoga@mcw.edu (N. Yoganandan).

Loading to the lateral region of the head, in contrast to the frontal bone, has been investigated less frequently in laboratory research and promulgated to a lesser extent from standards perspectives. Biomechanical side impact studies using intact human cadavers have routinely eliminated head injury assessment in the experimental protocol adding to the paucity of data for this region of the human body (Maltese et al., 2002; Pintar et al., 1997; Yoganandan et al., 2002). This is because these side impact studies, primarily applicable to vehicle environments, were conducted when effective countermeasures (e.g., side airbags) did not exist. Since the last decade, owing to increased public awareness for occupant safety, these types of impacts are being examined in greater detail by epidemiologists, clinicians, biomechanical investigators, and regulators around the world (Careme, 1989; Fildes et al., 1994; Gloyns et al., 1994; Lund, 2000; Zaouk et al., 2001). In May 2003, the federal Department of Transportation of the United States added a warning to its safety assessment of injuries in side impact (NHTSA, 2003). This was based on the observation that the head injury criterion (derived for frontal impacts) may exceed its limits when the side of the head contacts with the interior roof-rail-pillar structure of the vehicle. Thus, there is a need to examine the tolerance of the human head to side impact. Because the skull deforms secondary to loading and is a vital component that encloses the brain, it is necessary to understand its biomechanical role and tolerance in addition to the other components (Gennarelli and Meaney, 1996). Fracture being a primary consequence of skull deformation, this review emphasizes biomechanical fracture tolerances and injury criteria. A brief biomechanical anatomy of the side of the skull precedes tolerance estimations. Because a majority of papers in the area are not published in journals, attempts are made to provide numeric data and graphic output to facilitate analyses and are presented in a chronological order to maintain the history and sequence of the development of biomechanical research in the area.

2. Anatomy in brief

From a biomechanical perspective, the human skull bone lies inferior to the scalp, a connective tissue (Williams, 1995). It is composed of three layers: the outer and inner tables sandwiching a dipole layer (Fig. 1). Structurally, the dipole is soft, with material properties similar to the cancellous bone of the human vertebral column, and the two tables are relatively rigid, comparable to the cortices of the vertebrae or long bones (Agur and Lee, 1991). The geometry of the cranial vault is complex and three-dimensional. Generally, it is symmetric about the mid-sagittal plane. The skull bone develops with age. During early stages of development,

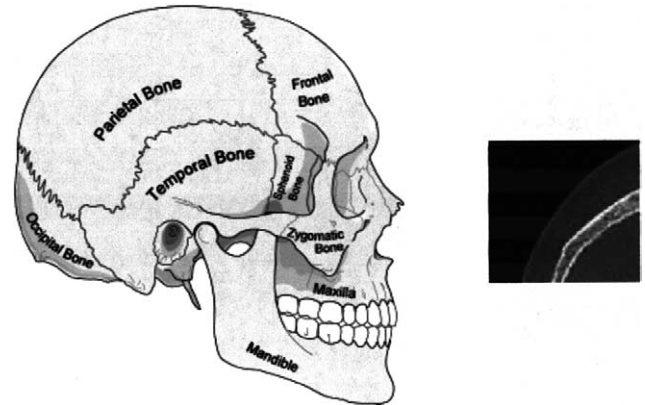


Fig. 1. (Left) Schematic view of lateral skull showing the various bones. (Right) Computed tomography section demonstrating the outer and inner tables of the temporo-parietal region of the human skull bone (brighter lines) sandwiching the dipole layer. Soft tissue density overlying the outer table is also visible.

it is composed of plates representing different regions, with cartilaginous components acting as connecting elements between the plates. The newborn skull is only approximately 4% stiff compared to the adult. It quickly matures attaining approximately 75% stiffness around 6–8 years (Kleinberger et al., 1998; Mohan et al., 1979; Yoganandan et al., 2000) the cartilaginous components, called fontanels, coalesce with age. The adult skull bone can be divided into frontal, rear (occipital), top (vertex), and side regions (Yoganandan et al., 2000). The side of the head can be further classified into the parietal (superior) and temporal (inferior) regions, shown in Fig. 1 (Tanner, 1962; Tindall et al., 1996; Youman, 1996). Although bones (e.g., hip and lumbar spine) are known to lose strength with advancing age, skull bones do not particularly show this behavior (Mosekilde and Mosekilde, 1986; Yoganandan et al., 1988; Yoganandan et al., 1998). This is because of the relatively larger proportion of the rigid cortical and the inner and outer tables. In contrast, brain material shrinks (atrophy) with advancing age. The thickness of the skull bone demonstrates regional variations. The temporal region is thinner compared to the parietal, occipital and frontal counterparts (Youman, 1996). Generally, the temporal region is concave inwards (medially) and the parietal region is convex. This changing geometry including thickness variations often challenges experimental investigators to accurately load or impact one region without engaging the other, one unlike the frontal bone. In side impacts, both regions are often involved in absorbing external force. Despite geometrical differences, these regions are constitutionally identical.

Dura separates the inner table from the brain. Inward bending of the skull resulting in dural laceration may lead to epi- or subdural hematoma (Gennarelli and Meaney, 1996).

3. Tolerance investigation

Biomechanical tolerance investigations can be classified into four categories: analyses of real-world events (e.g., athletic, fall, and motor vehicle), human volunteer experiments, animal tests and human cadaver studies, and mathematical simulations. Analysis of real-world events provides information on the injury and characteristics of the impact event, with little quantification of the actual biomechanical parameters (e.g., forces) responsible for the injury (CIREN, 2001). Human volunteer experiments, on the other hand, provide information only on sub-injury biomechanics (DeRosia and Yoganandan, 2000). Ethical and other reasons limit these studies to the injury domain. Animal tests provide physiological and injury data although scaling laws are necessary to translate to the *in vivo* human (Ommaya et al., 1967; Ommaya, 1985). Precise scaling laws do not exist. Mathematical simulations have the unique ability to perform parametric studies although validation must be based on experiments (Sances et al., 1981; Voo et al., 1996; Yoganandan et al., 1996; Yoganandan et al., 1987). Further, such simulations cannot determine injury tolerance, as failure criteria are not known for complex biological materials. In contrast, human cadaver experiments provide deterministic data on skull bones because of the anatomical equivalency with the *in vivo* human, and tests can be designed to subject the specimen to injury producing forces (Yoganandan et al., 1998). Therefore, this model is chosen for presentation. To determine the failure characteristics of the cranium, although studies have been conducted using isolated skull specimens (termed skull-caps), the review is mainly focused on intact head tests. To keep with the objective of the study, research with side impacts to the head are described at a greater length with comparisons from the other regions of the skull (e.g., frontal bone).

4. Early studies

Historical studies on head injury biomechanics, like the neck, began in mid-late 1800 (Duncan, 1874). In 1854, Bruns (cited in Messerer, 1880) compressed human heads with intact skin using a vise between two plates of wood along longitudinal (AP) and lateral directions (Messerer, 1880). Although forces were not recorded, alterations in the diameter were measured along and perpendicular to the loading direction using markers placed at desired locations. Poisson's effect was proved for skull deformations; compressive loading in one direction resulted in tensile deformations in the other perpendicular direction. Fractures were associated with the least out-bending curvature. For longitudinal

loading, fracture occurred at 11 mm of AP displacement and 5 mm of lateral extension. For lateral loading, fracture occurred at a displacement of 15 with 8 mm longitudinal displacement. In another head loaded to 13-mm deflection, a residual deformation of 2 mm was found. These results were compared in a later study, conducted by Baum in 1876 (cited in Messerer) that determined compressive properties of the human skull without skin using an iron ring (Messerer, 1880). Out of the three tested skulls, one fractured at 10 mm, and the second fractured at 7.5 mm secondary to lateral compression. The third skull tested in the longitudinal direction produced a fracture at 10 mm of displacement. The authors concluded that skin has no influence on biomechanical properties. In 1857, Hyrtl (cited in Messerer) reported that human heads "jumped like a ball," implying elasticity, secondary to drops from various heights (Messerer, 1880). Specimens painted in black were dropped onto white colored surfaces. The bouncing property was compared to drops of balls made out of elephant teeth; however, additional details were not given. In 1859, Cohnstein reported that pediatric heads were elastic secondary to compression (Cohnstein, 1875). The study, aimed at evaluating the effects of forceps compression on newborns, recorded changes in diameters in two perpendicular directions. Transverse diameters decreased, remained unchanged, or increased, and such phenomena occur secondary to immature skeletal plates. Adult skulls do not show this pattern because of ossification and fusion of cartilaginous structures (Yoganandan et al., 1995).

In 1880, Messerer conducted quasi-static compression tests in the lateral direction using 13 unembalmed human cadaver heads (seven males, 18–83 years, six females, 22–82 years), and reported fracture forces ranging from 400 to 600 kg for males and 300 to 800 kg for females (Messerer, 1880). Peak failure forces as a function of gender showed opposite trends between side (male lower than female, 489 kg \pm 84, 562 kg \pm 177) and frontal (male higher than female, 686 kg \pm 303, 610 kg \pm 143) sites (Fig. 2). For side (lateral) loading, mean failure deflections were lower for males (4.3 mm \pm 1.9) than females (5.7 mm \pm 1.8), although no statistical conclusions were drawn. However, such gender differences (male: 2.8 mm \pm 1.5 versus female: 2.8 mm \pm 0.9 mm) were not reported (Fig. 2) for frontal (AP) loading tests (seven male, five female, 19–74 years). These data indicate that the human skull is more compliant in the lateral than the AP region. For side loading, the actual force–deflection plots as a function of gender and on a specimen-by-specimen basis are shown in Fig. 3. These conclusions are applicable to static loading. To better understand the behavior of the human skull bone under impact, dynamic studies are needed, and later researchers conducted tests using this change in modality.

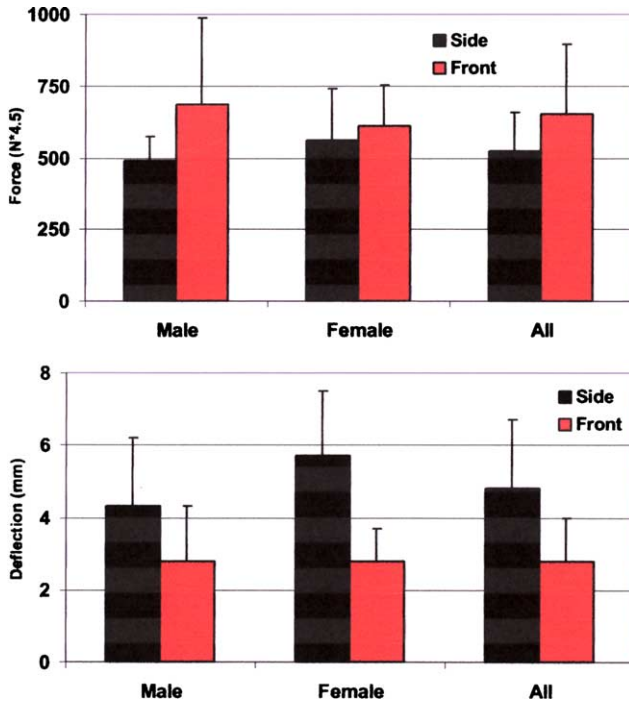


Fig. 2. Histogram of peak force (a) and deflection (b) comparing the two loading sites (data from the Messerer study).

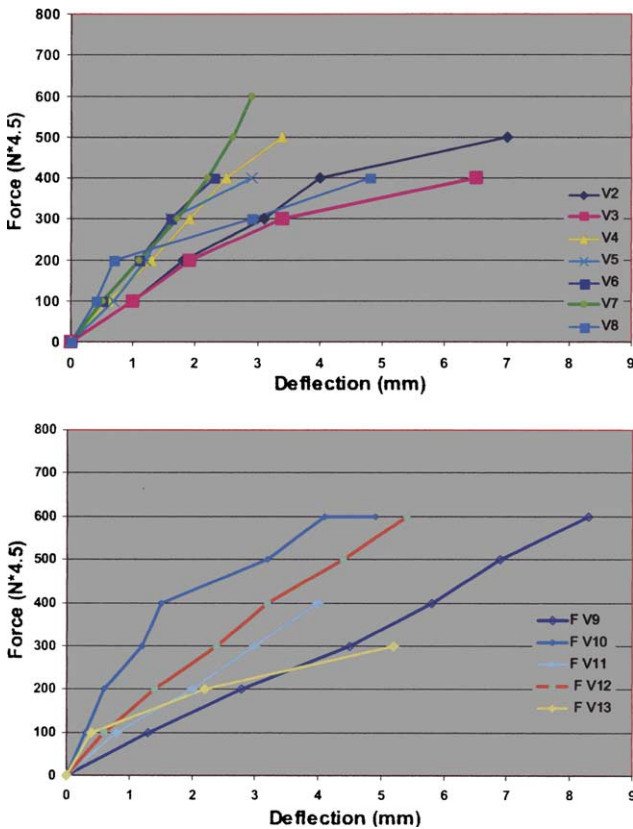


Fig. 3. Male (a) and female (b) specimen responses from the Messerer study. Specimen numbers used in the original publication are shown in legend.

5. Recent studies

In the 1940s, Gurdjian and co-workers conducted impact tests to investigate the mechanics of head injury (Gurdjian and Webster, 1946; Gurdjian et al., 1947, 1949, 1953). Embalmed intact human cadaver heads were dropped onto a solid steel slab (73 kg weight) and pathology and biomechanical data in the form of input external energy were reported (Gurdjian et al., 1949). Brittle strain sensitive lacquer that cracks in response to tensile strain (termed stresscoat technique) was used to identify pathology (Gurdjian and Webster, 1946). Linear fractures occurred secondary to tensile stresses caused by local skull bending due to impact. Lateral impacts consisted of focusing the anterior interparietal or left or right posterior parietal regions. Energies (drop height times head weight) for these two regions ranged from 801 to 1223 and 653 to 1230 Nm, and velocities ranged from 4.6 to 6.4 and 5.0 to 6.3 m/s (Fig. 4). Comparison of data (Table 1) from other regions indicated that the occipital region is the weakest followed by the mid-frontal, posterior parietal, and anterior interparietal regions. Variations (more for energy than velocity) were attributed to geometrical characteristics such as skull and scalp thickness and shape. Fracture thresholds for dry skulls were lower than intact heads indicating the lack of biofidelity of dry skulls for predicting human tolerance. Comparison of these data with static tests (Messerer, 1880) demonstrates loading rate effects. For example, the human parietal bone is stronger than the frontal bone under impact loading.

The actual contact area could not be measured in these drop tests because of a lack of instrumentation (no pressure sensitive film was available) and the study used

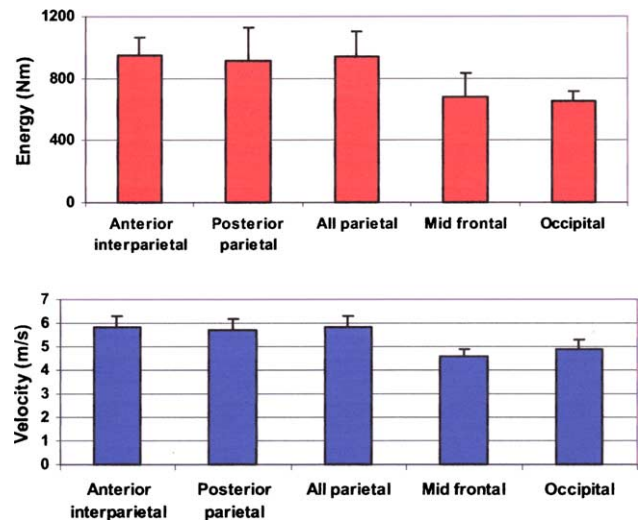


Fig. 4. Comparison of energy and velocity thresholds for fracture of intact human heads (data from Gurdjian et al.).

Table 1
Biomechanical data from the Gurdjian et al. study for all fractures

Region	Velocity (m/s)	Energy (N m)
Anterior parietal	5.8 ± 0.5	948.3 ± 120.1
Posterior parietal	5.6 ± 0.5	910.9 ± 219.0
All parietal regions	5.8 ± 0.5	943.0 ± 161.3
Mid frontal	4.6 ± 0.3	678.0 ± 156.1
Occipital	4.9 ± 0.4	652.6 ± 67.2
Anterior parietal	5.5 ± 0.8	963.3 ± 180.7
Posterior parietal	5.6 ± 0.2	833.1 ± 68.1
All parietal regions	5.3 ± 0.4	858.4 ± 54.9
Mid frontal	4.8 ± 0.4	773.7 ± 275.7
Occipital	4.8 ± 0.2	700.9 ± 28.8

intact cadaver head impacts onto rigid surfaces. To study the effects of contact area on skull bone tolerance, in 1968, Nahum and co-workers conducted a study wherein unknown velocity impacts (645-mm² contact area, 5-mm padding) were delivered using an impacting mass to the temporo-parietal junction of five unembalmed (55–75 years) and five embalmed (60–81 years) intact human cadaver heads (Nahum et al., 1968). The heads were supported using 10–13 cm styrofoam rubber. Varying combinations of impactor mass and drop height were used in the experimental design. Mean fracture forces for females (3123 ± 623 N) were lower than males (3944 ± 1287 N). These forces were lower compared to the fracture forces for the frontal bone

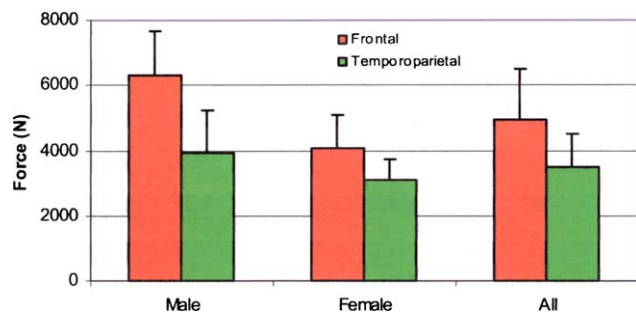


Fig. 5. Mean peak fracture forces (N) as a function of impact site (data from Nahum et al.).

Table 2
Side impact biomechanical data (Schneider et al.)

Description	Fracture (yes/no)	Mean force (N)	Velocity (m/s)
Intact cadaver	No	3792 ± 1865	5.3 ± 0.8
Isolated specimen	No	2886 ± 987	5.4 ± 0.3
All specimens	No	3248 ± 1418	5.4 ± 0.6
Intact cadaver	Yes	4208 ± 1013	5.9 ± 0.2
Isolated specimen	Yes	3351 ± 613	5.4 ± 0.3
All specimens	Yes	3630 ± 969	5.6 ± 0.4
Intact cadaver	Yes and no	4000 ± 1447	5.6 ± 0.6
Isolated specimen	Yes and no	3032 ± 858	5.4 ± 0.3
All specimens	Yes and no	3433 ± 1216	5.5 ± 0.5

(Fig. 5). Based on these data, minimum tolerance levels of 2450 N for males and 2000 N for females were suggested for the temporo-parietal bone for clinically significant fractures with an approximate contact area of 645 mm². Using the same specimen, tests were also conducted at the zygoma and mandible to determine their biomechanical responses; for brevity, these facial bone impact tolerance data are not reported here. While the above results are similar to the static tests of Messerer (1880), they are in direct contrast to Gurdjian’s drop tests wherein the frontal region was determined to be weaker (lower fracture force) than the side of the head (Gurdjian et al., 1949). However, it should be noted that these results are applicable to impacts delivered to a fixed area (of contact) to the frontal or temporo-parietal regions of the head. This group extended tests into the temporo-parietal region.

In the follow up study, Schneider and Nahum (1972), conducted additional temporo-parietal impact studies using intact (three embalmed, three unembalmed) and isolated head-C7 (five embalmed, four unembalmed) specimens. Intact cadavers were lying supine, and isolated specimens were supported by wedges of polyurethane padding. Weights (ranging from 1.1 to 3.8 kg) were dropped onto various regions at velocities ranging from 3 to 6 m/s. Injuries ranged from none to severe comminuted fractures. Table 2 shows a summary of peak forces along with impact velocities and specimen types (intact versus isolated). While the velocities are very similar for both models, considerable overlap exists in the data between intact and isolated specimens, suggesting the use of either model for determining skull tolerance to impact. Comparison of the temporo-parietal data with frontal bone tolerance from tests conducted by this group shows that peak forces for the two regions fall within the range of each other, implying similarities in fracture thresholds (Fig. 6).

In the 1960s and 1970s, Hodgson and co-workers undertook a series of investigations to determine human cadaver head tolerance to impact (Hodgson and Thomas, 1973, 1972; Hodgson et al., 1973). Frontal, lateral, occipital, and facial regions were considered

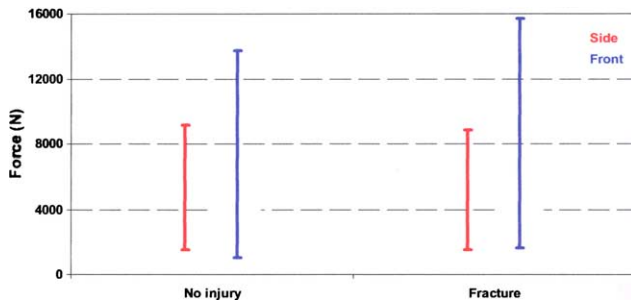


Fig. 6. Comparison in the range of fracture forces between frontal and temporo-parietal impacts from embalmed and unembalmed intact and isolated human cadavers (data from Schneider et al.).

(Hodgson, 1967; Hodgson and Thomas, 1971). In 1971, results were reported from 35 drop tests conducted with seven embalmed human male cadavers with age from 45 to 83 years, height from 173 to 180 cm, and weight from 50 to 102 kg (Hodgson and Thomas, 1971). Head weight ranged from 3.8 to 5.9 kg (mean 4.4 ± 0.7). Two pairs of bi-axial accelerometers were glued to the skull to record transverse and antero-posterior accelerations. A load cell mounted under the rigid impact surface recorded the dynamic force. The head was restrained by a cord from rotating into the preferred position during free fall. The cadavers were raised to the desired height above the surface and dropped from a height of 12.7 to 114.3 cm (1.6–4.7 m/s impact velocity) in steps of 12.7 cm to contact a rigid flat plate. Multiple drops were conducted on each specimen. One specimen was dropped on the left side four times (12.7–50.8 cm) and on the right side nine times (12.7–114.3 cm) without fracture. All other six specimens exhibited linear fractures. Peak impact forces ranged from 5560 to 17792 N (mean 10151 ± 4928), and peak antero-posterior accelerations ranged from 190 to 325 g (mean 267 ± 71). Antero-posterior accelerations were reported in four impacts. Pulse times ranged 2.5–6 ms (mean 4.6 ± 1.5). These values were lower than the values found from frontal impact tests (Table 3).

At a lower drop height of 12.7 cm, the shapes of the biomechanical responses were half sine. In contrast, drop heights greater than 63.5 cm did not produce such clear trends. Skull thickness measurement was not adequate to characterize the skulls because of large varia-

tions in shape, blood vessel erosion, foramina, sinus cavities, and table geometry. A comparison of these side impact force and acceleration data with their companion study on rear and frontal bones indicated the skull to be the strongest in the posterior (rear), followed by the lateral (side) and AP (frontal) regions (Fig. 7). Results

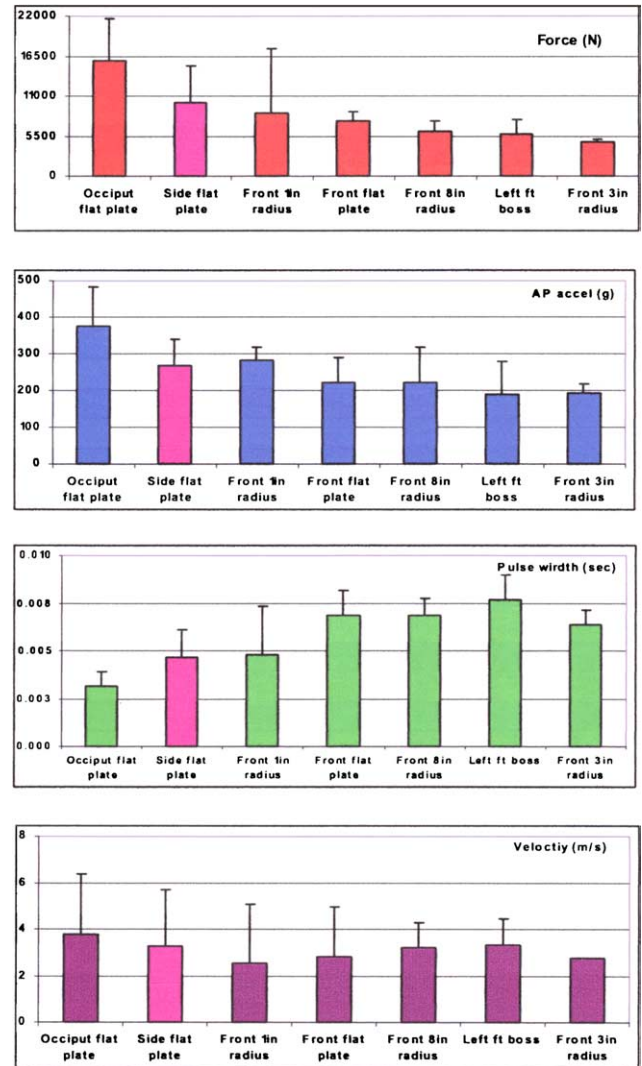


Fig. 7. Comparison of biomechanical responses of intact human cadavers (data from Hodgson et al.). Side impacts with the flat plate are emphasized in the same color in all plots.

Table 3
Mean fracture forces from intact human cadaver impacts (Hodgson)

Region—impact surface	Peak force (N)	Pulse width (s)	AP acceleration (g)	Impact velocity (m/s)
Occiput—flat plate	15902	0.0031	375.0	3.75
Side—flat plate	10151	0.0046	267.5	3.27
Front—1 in radius cylinder	8718	0.0048	281.0	2.55
Front—flat plate	7636	0.0068	222.5	2.81
Front—8 in radius hemisphere	6183	0.0068	222.0	3.24
Frontal boss—1 in radius cylinder	5827	0.0077	191.0	3.31
Front—3 in radius hemisphere	4604	0.0064	193.8	2.73

were not conclusive with regard to the effect of contact area, i.e., increase in area contributing to decreased forces. Because all cadavers were impacted onto rigid surfaces, to better describe the mechanics, the authors recommended repeating their study with deformable surfaces. Because the head injury criterion was advanced later, HIC values are not available (Versace, 1971).

In 1972, McElhaney et al. reported data from sub-failure quasi-static tests conducted using unembalmed intact human cadavers (McElhaney et al., 1972). The head was positioned between two steel platens (150-mm diameter) and loaded using a materials testing device. Force–deflection curves from loading to the temporal (50 mm above the auditory meatus) and frontal (100-mm diameter impactor and point of loading located 50 mm superior to the glabella) regions were reported from 12 tests for each site. The 23 cadavers ranged from 48 to 99 years of age (three females, 20 males). Head and brain weights ranged from 3.8 to 5.5 kg and 1.2 to 1.4 kg. From the non-linear force–deflection responses, bilinear approximations were made, and the stiffness in the second region ranged from 700 to 1750 N/mm for the temporal and 1400 to 3500 N/mm for the frontal regions. Twelve tests were conducted for each site. Significant overlap existed (Fig. 8) in the response between the two anatomical sites. Further, both sites responded with forces in the 4000–8000 N range although tests were non-destructive.

In 1977, left lateral impacts were conducted on unembalmed human cadavers seated in the upright position using a pneumatic piston at velocities ranging from 6 to 9 m/s (Stalnaker et al., 1977). A portion of the scalp was removed, exposing the skull for placing the instrumentation. Accelerometers potted in dental acrylic were positioned by the aluminum jig to ensure the mutual orthogonality with the three Cartesian axes. The cadaver was seated in an upright position in an adjustable chair. The head and torso were stabilized by fastening a wax cord to each auditory meatus and attaching cords to an overhead support structure. A five-liter fluid-filled container was connected to the cadaver's pressurization

tube and to an air supply. The air pressure was increased until a steady vascular pressure of 120 mm of mercury was reached. Impacts were conducted using a pneumatic testing machine consisting of an air reservoir and a ground and honed cylinder. A transfer piston propelled by compressed air transferred (its) momentum to the impact piston. A striker surface with an inertially compensated load cell was attached to the piston for measuring the applied force. The impact piston and load cell striker assembly had a mass of 10 kg, and the striker was 15.2 cm in diameter. Autopsies were conducted following impact and injuries were classified according to the Abbreviated Injury Scale, 1976 version (AIS, 1990). Anthropomorphic measurements included the length and breadth data, defined as maximum inside dimensions of the skull. The average thickness of the skull was determined from measurements of the front, side, and rear of the skull. Circumference was obtained at the anatomic level of the length and breadth measurements. Impact forces, accelerations, and durations were reported for each specimen. Pulse duration was obtained by linear regression interpolations to the loading and unloading regions of the responses.

Three padded (25.4-mm Ensolite) and two rigid impacts were conducted on one male and four female cadavers with age, height, and weight ranging from 54 to 78 years (67.2 ± 8.9), 152 to 179 cm (mean 164 ± 10.4), and 44 to 83 kg (mean 63.6 ± 20.9). Peak forces and accelerations ranged from 4.21 to 9.59 kN (mean 6.1 ± 2.3) and 125 to 532 g (mean 247 ± 169). All three drops with padded surfaces did not result in bony pathology with peak forces ranging from 4.2 to 4.8 kN and peak accelerations from 125 to 179 g. However, both rigid drop specimens sustained AIS 3 fractures; temporal and occipital bones in one case at a peak force of 7.15 kN and acceleration of 262 g, and a comminuted fracture of the temporal bone at a peak force and acceleration of 9.6 kN and 532 g in another case. Impact velocities were 7.2 and 6.8 m/s for these two impacts. As expected, padded impacts produced lower forces and accelerations than rigid impacts. In addition, pulse durations were considerably lower. Comparison with other studies with regard to the HIC variable is not possible because of lack of data. These results suggest that impacts to the side region of the head can sustain approximately 5 kN of impact force without causing skull fracture. Data from these tests are summarized (Table 4). A comparison of side impact data with results from rear impacts conducted using the same experimental protocol revealed that the occipital bone fractures at a force of 9.61 kN, pulse duration of 2.198 ms, at a velocity of 6.3 m/s for a 75-year-old female cadaver (169-cm tall and 76.2-kg body weight). Other cadaver impacts at the rear or frontal region did not result in skull fractures. However, padding decreased peak forces.

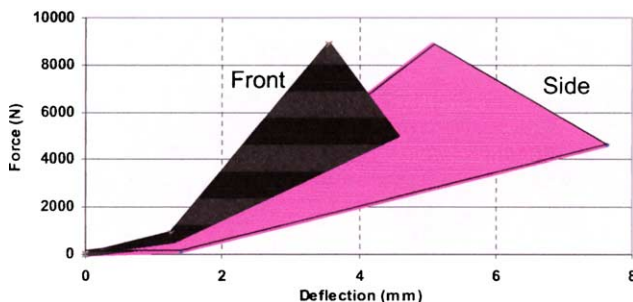


Fig. 8. Quasi-static force–deflection responses of side and frontal loading to intact human cadavers (data from McElhaney et al.). Stiffness in the second portion shows overlap between the two anatomical sites.

Table 4

(a) Subject demographics (Stalnaker et al.); (b) biomechanical data and (c) comparison of biomechanical data for different impact sites

ID	Age (years)	Gender	Height (cm)	Weight (kg)	Padding
<i>(a) Subject demographics (Stalnaker et al.)</i>					
75A113	54	Male	179	83.0	25 mm Ensolite
75A116	66	Female	152	44.0	25 mm Ensolite
76A134	72	Female	170	47.2	25 mm Ensolite
76A145	78	Female	160	80.3	Rigid
76A152	66	Female	160	–	Rigid
	Peak force (kN)	Duration (ms)	Velocity (m/s)	Acceleration (g)	Skull fracture
<i>(b) Biomechanical data</i>					
75A113	4.82	9.7	5.97	124.8	None
75A116	4.65	9.1	9.08	178.8	None
76A134	4.21	10.6	6.20	137.1	None
76A145	9.59	6.9	6.82	532.0	Temporal comminuted
76A152	7.15	6.9	7.17	262.3	Occipital and temporal
Impact site	Fracture, yes/no (AIS)	Mean peak force (kN)	Impact velocity (m/s)	Peak acceleration (g)	
<i>(c) Comparison of biomechanical data for different impact sites</i>					
Side	No	4.56 ± 0.31	7.08 ± 1.73	146.9 ± 28.3	
Side	Yes (3)	8.37 ± 1.73	7.00 ± 0.25	397.5 ± 190.7	
Front	No	8.67 ± 3.35	5.97 ± 0.29	247.7 ± 150.9	
Rear	No	9.93 ± 0.83	7.41 ± 1.19	204.3 ± 43.6	
Rear	Yes (3)	9.61	6.35	359.3	

Only one specimen showed fracture for rear impact case.

In 1978, European investigators quantified the temporo-parietal responses from five intact human cadavers subjected to 19 rigid and padded impacts (Got et al., 1978). The subjects were suspended in a metal cradle and oriented at angles ranging from 18° to 35°. The unit was released to accomplish a free fall. The head and upper part of the thorax protruded beyond the table such that the temporo-parietal region of the head sustained the impact force. The circumference and length of the head were measured over the lowest part of the frontal bone and the outer occipital protuberance. The width of the head was defined as the maximum distance between the right and left parietal–temporal regions. Accelerometers on the frontal bone, occiput, and right temple gathered data. Accelerations of the center of gravity of the head were computed. The impact force was recorded using a load cell. Cadavers were perfused using one volume of India ink, three volumes of formaldehyde at 30%, and six volumes of water. The total volume injected was three liters. In addition, the arterial system was pressurized. Three drop heights were used: 1.83 m according to the FMVSS 218, 2.5 m according to the French standard, and 3 m. After testing, the head, neck, skull, and frequently the brain were weighed, and soft and hard tissue injuries were identified using gross dissection and histology.

Two rigid impact tests produced peak forces of 12.2 and 12.5 kN, and three tests with padded impact produced peak forces ranging from 5.0 to 10.1 kN (Table 5a). Although no fractures were identified in

padded impacts, both specimens in rigid impacts sustained (minor in one and “very large” in the other) skull fractures. In one rigid impact, head injury criterion (HIC) exceeded 7000 with frontal accelerometer data and exceeded 1700 with right temporal accelerometer data. The use of the contralateral accelerometer produced minimal variations in HIC while the use of computed center of gravity accelerations increased the HIC by a factor of 2.5; the force increased by approximately 25% (Table 5b). In addition, HIC computed from the accelerometer placed on the right side did not exhibit the same tendency (high or low) when compared with the HIC from sensors placed at other anatomic locations or computed at the center of gravity. However, HIC computed from the center of gravity accelerations were always lower than those computed from the frontal accelerometer. In-bending of the cranial bone at the impact site results in a hoop-type distraction at the anterior and posterior regions, and this deformable behavior contributes to variations in the acceleration responses and resulting HIC values. Computations of accelerations at the center of gravity and HIC by assuming the head to be a rigid body during fracture producing high-velocity impacts are only a first approximation. In addition, although the use of formaldehyde as a fixative minimizes autolysis and facilitates histological analysis, because the process induces (partial) embalming, results may not be completely applicable to unembalmed specimens or in vivo situations.

Table 5

(a) Subject demographics (Got et al.); (b) biomechanical data and (c) comparison of biomechanical data for different impact sites

ID	Age (years)	Gender	Height (m)	Head weight (kg)	Circumference (m)	Lateral breadth (m)	AP length (m)	Padding (mm)
<i>(a) Subject demographics (Got et al.)</i>								
68	49	Female	1.8	3.82	0.556	0.145	0.184	None
76	75	Male	2.5	3.45	0.550	0.140	0.192	None
145	68	Male	3.0	3.45	0.545	0.150	0.180	36
146	68	Male	3.0	3.90	0.548	0.150	0.180	36
147	57	Female	3.0	3.59	0.538	0.140	0.190	36
ID	Peak force (N)	Velocity (m/s)	HIC from right accelerometer	HIC from frontal accelerometer	HIC from rear accelerometer	HIC from cg	Skull fracture	
<i>(b) Biomechanical data</i>								
68	12,200	5.99	1700+	7000+	–	7000+	Minor	
76	12,500	7.00	2531	5196	4200	5000	Very large	
145	10,100	7.67	2428	2318	–	2000	None	
146	6,900	7.67	1911	1315	1114	1200	None	
147	5,000	7.67	1695	1045	592	800	None	
Impact site	Fracture (yes/no)	Mean peak force (N)	Impact velocity (m/s)	Acceleration (g)				
<i>(c) Comparison of biomechanical data for different impact sites</i>								
Side	No	8500 ± 2263	7.67 ± 0.0	146.9 ± 28.3				
Side	Yes	12350 ± 212	6.50 ± 0.7	397.5 ± 190.7				
Front	No	8500 ± 3807	7.67 ± 0.0	247.7 ± 150.9				

Note: Data from ID 147 rejected because the brain was “very flabby.”

Impact tests using the frontal bone as the site of loading (7.67 m/s velocity) produced no fractures (six specimens). Peak forces ranged from 5.6 to 14.0 kN. HIC computed using the center of gravity acceleration data were 1000 and 2800 for two specimens (forces 5.6 and 6.0 kN). HIC computed using rear accelerometer signals ranged from 1022 to 3870. The force data match very well with such data for the side loading suggesting the overlap phenomenon between the fracture thresholds for these sites. However, such clear conclusions could not be drawn for fracture tests because of differences in impact velocities (Table 5c). Biological variability and lack of sufficient sample size offer explanations for this issue.

In a later study, these investigators reported very poor correlations ($R < 0.2$) between age, cranial vault dimensions, and fracture force (Got et al., 1983). Higher correlations were found between vault weight and mineralization expressed by surface units ($R = 0.74$). Skull bone condition factor, defined using the thickness of the skull, skull diameter, skullcap mineralization, and head mass correlated well with mechanical tests performed on skullcap fragments.

In 1980, Nahum et al. conducted tests using one embalmed intact human cadaver (four impacts) and five unembalmed cadavers (one impact to each cadaver) using a rigid mass (4.17 kg) at velocities ranging from 6.5 to 7.5 m/s for the embalmed cadaver and from 7.0 to 10.2 m/s for unembalmed cadavers (Nahum et al., 1980).

The mean age of the cadavers for both sexes was 73 years. The Frankfort plane was maintained horizontal, and padding materials (Ensolute or polystyrene padding, 3-cm thick) were inserted between the temporo-parietal region of the head and impactor to vary pulse durations. Peak head accelerations correlated well with HIC (334–1466 for embalmed and 1340–5246 for unembalmed cadaver tests, Fig. 9). The time interval maximizing HIC was considerably lower for unembalmed than embalmed cadaver tests (Table 6). Peak head accelerations linearly correlated ($R^2 = 0.86 - 0.99$, plot not shown) with positive pressures in the right frontal area near the region of impact ($R^2 = 0.99$). Pressures in the brain were recorded by piezoresistive transducers, threaded to the skull at various locations so that the diaphragm of the transducer communicated with the subdural space. Although a forensic pathologist examined the head and neck, descriptions of injuries were not reported, and hence, it is difficult to comment on human tolerance.

The invariant behavior of contact area with peak force was not observed in a later series of experiments. In 1991, Allsop et al. conducted impact tests on 31 isolated unembalmed cadaver heads with age ranging from 31 to 90 years (Allsop et al., 1991). The specimens were impacted using a flat rectangular plate (5 × 10 cm, 12 kg) or a flat circular plate with a contact surface diameter of 2.54 cm (10.6 kg). The impactors were fixed to a drop tower. Rectangular plate impacts were conducted at an impact velocity of 4.3 m/s, and circular

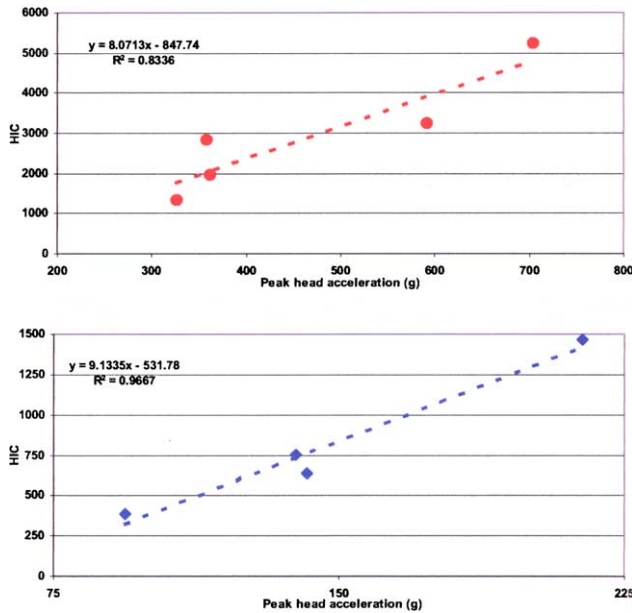


Fig. 9. HIC versus peak head acceleration plots from four tests on one unembalmed (a) and one test on each of the four unembalmed cadavers (data from Nahum et al.). Data points from each test are also shown.

plate impacts were conducted at 2.7 m/s. Displacements were recorded by two string potentiometers attached to the impacting mass. Forces were recorded using a Kistler load transducer for the circular plate tests and piezoelectric transducers for the rectangular plate tests. Fracture detection was accomplished by attaching conical shaped wave-guides to a 6.4-mm diameter acoustic emission sensor through a skin incision near the impact site. Two locations on the temporo-parietal regions were selected for the circular impactor. For the rectangular impactor, the parietal region was selected as the impact site. The mean fracture for rectangular plate impacts was 12390 N (± 3654). The average fracture force for

both impact sites with the circular impactor was 5195 N (± 1010). Stiffness was computed as the average slope of the force–displacement curve between 4 and 12 kN for the rectangular plate impactor and 2–6 kN for the circular plate impactor. Rectangular plate impactor tests responded with stiffness ranging from 1600 to 6430 N/mm (mean 4168 ± 1626). Circular plate impactor tests resulted in stiffness values ranging from 700 to 4760 N/mm (mean 1800 ± 881). Although the bone mineral content (expressed traditionally as mg/cc) was not reported on a specimen-by-specimen basis, the authors concluded that the relationship between mineral content and fracture force was not significant, and calcium or magnesium content do not affect the fracture force. The contact area of the impactor significantly affected peak forces. Hodgson and Thomas (1971) and Yoganandan et al. (1993, 1991a, 1989, 1991b) advanced similar conclusions on facial bone structures in experimental studies in 1970s and 1980s. Because of the complex anatomy of the lateral side of the head, while experiments can be conducted to control the impacting region, partial (to full) involvement of the parietal region occurs in the real world. Consequently, failure biomechanical data may be bound by the temporal and parietal regions with the former acting as a lower and the latter serving as an upper bound.

In 1993, McIntosh et al. conducted lateral impacts to 11 unembalmed cadavers using a 25–28 kg, 150-mm diameter aluminum impactor. Age ranged from 22 to 77 years (four female, seven male). The cadaver was placed on a seat that supported backs up to the level of the scapula. The head was positioned in the neutral position, and the impactor was aligned to the junction between the parietal and temporal bones superior to the auditory meatus. Tests at velocities ranging from 3.9 to 6.1 m/s (undamped impacts) were conducted without padding and from 2.8 to 3.8 m/s were conducted with 2.54 Ensolite padding in front of the impactor. Skull

Table 6

(a) Repeated tests from one embalmed human cadaver (Nahum et al., 1980) and (b) single impact tests from four unembalmed human cadavers

ID	Padding type and thickness	Impact velocity (m/s)	Peak acceleration (g)	HIC	t_1 (ms)	t_2 (ms)	Δt (ms)
<i>(a) Repeated tests from one embalmed human cadaver (Nahum et al., 1980)</i>							
70 W	Ensolite 3 cm	6.55	141.7	639	5.9	11.2	5.3
71 W	Ensolite 3 cm	7.54	214.1	1466	7.6	11.8	4.2
72 W	Ensolite 3 cm	7.54	138.6	752	5.7	11.2	5.5
73 W	Ensolite 3 cm	6.55	93.8	388	5.9	13.7	7.8
<u>Velocity (m/s)</u>							
<i>(b) Single impact tests from four unembalmed human cadavers</i>							
74 W	Ensolite 3 cm	8.05	361.9	1973	7.8	11.3	3.5
75 W	Ensolite 3 cm	7.03	326.2	1340	6.2	7.9	1.7
76 W	Ensolite 3 cm	8.83	703.4	5246	5.7	6.5	0.8
77 W	Ensolite 3 cm	9.68	357.8	2844	8.9	12.1	3.2
78 W	Polystyrene 1.0 cm	10.16	591.2	3249	9.1	10.1	1.0

Table 7
Side and occipital impact data (McIntosh et al.)

Site	Number of impacts	Velocity (m/s)	Peak force (N)	Skull AIS	HIC	Peak cg acceleration (g)
Side	10	4.6 ± 1.4	5979 ± 1946	0	1114 ± 1168	192 ± 116
Side	3	6.0 ± 0.1	11388 ± 363	2.3 ± 0.6	2925 ± 982	411 ± 119
Occipital	4	3.3 ± 0.5	5086 ± 1331	0	216 ± 116	82 ± 21
Occipital	4	4.9 ± 0.9	7272 ± 2657	3.5 ± 0.6	5011 ± 262	419 ± 174

fractures occurred in three cadavers with AIS rating ranging from 2 to 4. All these cadavers were subjected to undamped impacts at >4.0 m/s. As can be seen from Table 7, peak biomechanical parameters were lower in specimens with no injury (AIS = 0) compared to injured specimens. It should be noted, however, that only three specimens sustained skull fractures and the impact velocities were considerably higher than the ten specimens exhibiting no skull fracture. In this study, head weights were scaled according to procedures outlined by Reynolds, who reported the mass of the 50th percentile male head to be 3.98 kg (Reynolds et al., 1975). It should be noted that the SAE uses a mass of 4.69 kg for the 50th male. Difficulties were acknowledged in estimating the head center of gravity accelerations from the nine accelerometer array because of skull deformations at the instrumentation site, rigid body assumptions, and changing center of gravity during impact. To minimize high-frequency skull vibrations affecting angular accelerations, the authors reprocessed the data with a 200 Hz, 3 db cutoff filter. Because of the lack of sample size, data from occipital impacts (four fracture, four non-fracture) were grouped with side impact data and risk curves were developed using logistic regression analysis. At the 200 Hz filter level, a HIC value of 800 represented 50% injury risk. This analysis needs revision if regional tolerances of the occipital and lateral regions of the skull bone are not identical.

In a later study, Yoganandan et al. (1995) conducted controlled impacts using an electro-hydraulic testing device. In this research, the investigators fixed the inferior end of the intact head using a custom-designed device, and static and dynamic loads were delivered with the piston of the electro-hydraulic testing apparatus. Failure forces were 5292 and 5915 for the two parietally loaded specimens and 6182 N for the temporally loaded specimen. Failure deflections for these specimens were 8.9, 7.8, and 15.4 mm, respectively. Stiffness, defined as the slope in the most linear region of the force–deflection curve, was 695, 1143, and 487 N/mm. These data indicate that the parietal region is stronger (higher peak force) than the temporal region, although the temporal bone is more compliant (higher deflection). Temporal and parietal fractures were reported. Although tests at dynamic rates were not conducted at these anatomical sites, a comparison of static (at a rate of 0.002 m/s) and dynamic (8.0 m/s) loading (using data from other re-

gions, vertex, frontal, etc.) indicated that force tolerance increases by approximately a factor of two under dynamic loading. While X-rays and computed tomography scans identified skull fractures, the precise location and direction of the impact on the skull were not apparent in these images. The authors concluded that, based on retrospective imaging, it may not be appropriate to extrapolate the anatomical region that sustained the external insult. Because the experimental design included monitoring forces and deflection, actual force–deflection plots were provided, and the reader is referred to the original publication for graphical output.

6. Injury criteria

Based on these experiments, several candidates (peak forces, peak acceleration, Gadd severity index, and head injury criterion) exist for head injury quantification. The Society of Automotive Engineers (SAE, 1980 version) specifies peak force data in its specification (Society of Automotive Engineers, 1980). As can be seen from Fig. 10, sufficient overlap exists in the values between

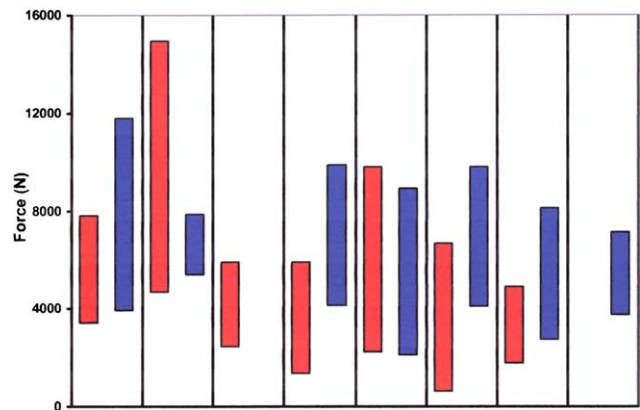


Fig. 10. Side (red) and frontal (blue) tolerance data from various experiments. (For interpretation of colour the reader is asked to refer to the web version of this article.) Each cell represents a separate study in the following sequence (from left to right): Messerer (unembalmed, flat plate), Hodgson (embalmed, flat plate), Schneider (unembalmed, 2.9 cm diameter impactor diameter), Schneider (embalmed, 2.9 cm diameter impactor diameter), Melvin (embalmed, 1.1 cm impactor diameter), Melvin (embalmed, 1.5 cm impactor diameter), Messerer (unembalmed, 1.7 cm impactor diameter), and Nahum (embalmed, 2.9 cm impactor diameter). Each bar represents the range in the experimental data for the side and frontal bones of the human head.

side and frontal impacts. In addition, ranges in the force data demonstrate overlap for various contact areas and cadaver preparations. The 1994 version of the SAE J1460 specifications, human mechanical characteristics, provides tolerance data as a function of contact area for the human head derived from literature (SAE, 1994). During the preparation of this specification, Hodgson reanalyzed experiments conducted in his laboratory, repeated some of his earlier tests, and revised his original results. The SAE corridors for fracture thresholds of the human head to flat impact surfaces (including this revision) as a function of contact area are shown in Fig. 11. The figure has been redrawn to include one full standard deviation instead of the one-half standard deviation plotted in the original SAE publication. These corridors are a first step in the understanding human tolerance.

Peak linear acceleration has been adopted by agencies such as the Snell and Canadian Standards for helmet applications (Canadian Standards Association, 1985; Snell, 1995). Peak linear acceleration associated with dwell times are suggested for motorcycle helmet standards by the US federal government (NHTSA, 1988). The severity index (also termed the Gadd severity index), uses an integral of the resultant acceleration response (Eq. (2)) measured at the center of gravity of the head (Versace, 1971). This index is used in football helmet standards (NOCSAE, 1997). Other indices such as the rotational acceleration and head injury power have also been proposed, although standards have not been promulgated using these proposals (Ommaya, 1985). The reader is referred to these publications for the limiting values of the index, acceleration level, and time intervals. The widely used head injury criterion, shown in Eq. (2), replaced the severity index (Versace, 1971). In the interest of brevity, arguments leading to the replacement of the index in vehicular impacts are not discussed. However, the head injury criterion is also

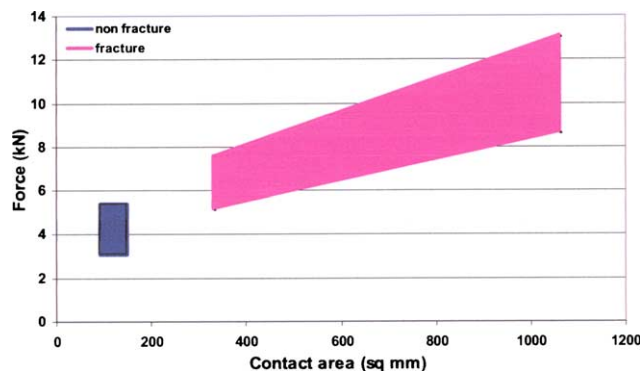


Fig. 11. Head impact response to flat rigid surface (SAE J1460). Peak forces for non-fracture are shown in blue and for fracture are shown in magenta color. (For interpretation of colour the reader is asked to refer to the web version of this article.) Shaded area represents mean plus or minus one standard deviation. See text for details.

based on the integral of the resultant acceleration at the center of gravity of the head, and remains as the most widely used metric for frontal impact crashworthiness assessment around the world (NHTSA, 2002). The criterion uses time-averaged, weighted acceleration data, and represents the kinetic energy transfer over a selected period. Based on the argument that HIC depends on the impacting boundary condition, another index termed skull fracture correlate (SFC, Eq. (3)) has been proposed more recently for frontal impacts (Van der vorst et al., 2003). However, for side impacts, the dependence of HIC on the impacting boundary condition is not experimentally evaluated. The skull fracture correlate uses the resultant acceleration at the center of gravity of the head in its determination. All these indices are derived or validated based on skull fracture tolerance to frontal bone impacts. If these criteria are identically used for the lateral impacts to the head, it is important to show that they are equally applicable; if the human skull shows regional dependency, there is a need to derive separate threshold(s) representing the lateral side of the human head.

$$SI = \int [a(t)]^{2.5} dt \quad (1)$$

$$HIC = \text{Max} \left[\frac{1}{(t_2 - t_1)} \int_{t_1}^{t_2} a(t) dt \right]^{2.5} (t_2 - t_1) \quad (2)$$

$$SFC = \left[\frac{\int_{t_1}^{t_2} a(t) dt}{(t_2 - t_1)} \right] \quad (3)$$

where $a(t)$ represents the resultant acceleration at the center of gravity of the head, and t_1 and t_2 denote the time interval that maximized the HIC criterion. A value of 1000 is considered to be the HIC limit. In contrast, SFC is a probability-based index representing 15% probability of frontal skull fracture at a value less than 120 g, and a 95% confidence band of 88–135 g.

7. Conclusions

The objective of this review was to present the findings from research studies with a focus on skull fracture in lateral impacts to the human head. A variety of variables have been included in the experimental protocols. Studies have used different loading conditions: quasi-static manual vise compression to electro-hydraulic materials testing device (piston) compression, dropping specimens onto a surface or dropping weights onto specimens, impacting specimens with padded and unpadded strikers and electro-hydraulic testing device (piston), and at varying velocities. Models have used intact cadavers, isolated heads with intact brain, and pieces of skull specimens. Unembalmed, partially embalmed, and fully embalmed conditions have been used

during specimen preparation. Loading paradigms have included single and repeated force applications. Biomechanical data have been gathered using force plate, linear variable differential transformer, and accelerometers. Data processing methods have included determinations of peak force, deflection, energy, stiffness, HIC, SFC, and acceleration. Lateral impact data have been compared with data from occipital, frontal, and facial bones. Some studies have focused on the temporal, parietal, and temporo-parietal regions, thus, providing data on the local anatomic differences. Consequently, a direct one-to-one comparison should not be made between studies without acknowledging these variables. However, certain general conclusions can be drawn from these investigations.

The human temporo-parietal region of the skull fractures similarly to the frontal and occipital bones because of their constitutional similarity (dipole sandwiched by the tables). Fracture threshold expressed in terms of parameters such as force overlap with the other region (frontal bone) although the mean force to fracture may be lower compared to the frontal bone. Because several studies were conducted prior to the advancement of the current widely used head injury criterion (US, Australian, Japanese, and European standards), data from all studies do not permit the evaluation of the index with frontal bone impacts. It is well known that the human skull is deformable, and the degree of deformability increases with impact severity, velocity for example (Wood, 1971). Accelerometers placed at the periphery of the human head can be used to compute the accelerations at the center of gravity of the head (Padgaonkar et al., 1975). This entails the determination of the center of gravity of the head, a parameter not accurately measured in every study. In some research, data from literature were used for the determination, thus introducing approximation (Becker, 1972; Beier et al., 1980; Walker et al., 1973). The importance and sensitivity of the determination of the center of gravity of the head to compute secondary variables such as HIC are well known in impact biomechanics. Furthermore, the computation incorporates rigid body assumptions, more applicable for low-velocity non-fracture tests than higher severity fracture-inducing impacts. Violation of the rigid body assumption affects biomechanical output. In addition, insufficient instrumentation (example, nine accelerometer package) used in previous studies precluded accurate computations of secondary biomechanical variables such as HIC. Consequently, additional research incorporating more instrumentation accounting for rotational accelerations and accurate determination of the center of gravity of the head are needed to better define the tolerance of the human skull to lateral impact. Because skull deformation affects the motion of the brain tissue, additional studies are needed to replicate side impact-induced head

injury and determine head injury tolerance in side impacts. Only when these variables are fully quantified, will there be a reason to adopt the same, merge one or more, or specify different tolerances to different regions of the human head including the temporo-parietal region. Because the human brain is more susceptible to trauma when the impact vector is aligned along the lateral rather than the antero-posterior direction, accurate quantification of the skull and brain responses in this mode are critical to predict injury, derive tolerance, design and develop and evaluate injury mitigating components (e.g., side airbags), and treatment paradigms.

Acknowledgements

This study was supported in part DTNH22-03-H-07147 and VA Medical Research.

References

- Agur, A.M.R., Lee, M.L., 1991. Grant's Atlas of Anatomy, 9th edition. Williams and Wilkins, Baltimore. p. 650.
- AIS, 1990. The Abbreviated Injury Scale. American Association for Automotive Medicine, Arlington Heights, IL, p. 74.
- Allsop, D., Perl, T., Warner, C., 1991. Force/deflection and fracture characteristics of the temporo-parietal region of the human head. In: Proceedings of the 35th Stapp Car Crash Conference, San Diego, CA.
- Becker, E., 1972. Measurement of mass distribution parameters of anatomical segments. In: Proceedings of the 16th Stapp Car Crash Conference, Detroit, MI, pp. 160–185.
- Beier, G., Schuck, M., Schuller, E., Spann, W., 1980. Determination of physical data of the head. I. Centre of gravity and moments of inertia of human heads. In: Proceedings of the IRCOBI, Troy, MI.
- Canadian Standards Association, 1985. Standard CAN3-D230-M85. Protective headgear in motor vehicle applications.
- Careme, L., 1989. Biomechanical tolerance limits of the cranio-cervical junction in side impacts. In: Proceedings of the International Congress and Exposition, Detroit, MI, pp. 55–70.
- CIREN, 2001. Crash Injury Research and Engineering Network-Program Report. NHTSA, Washington, DC.
- Cohnstein, 1875. Ueber Zangen application bei Beckenege. Arch. Path. Anat. Physiol. 64, 82–101.
- DeRosia, J., Yoganandan, N., 2000. Lessons from staged rear-end collisions using human volunteers. In: Yoganandan, N., Pintar, F. (Eds.), *Frontiers in Whiplash Trauma: Clinical and Biomechanical*. IOS Press, The Netherlands, pp. 265–294.
- Duncan, J., 1874. Laboratory note: On tensile strength of fresh adult foetus. Brit. Med. J. 2, 763–764.
- Fildes, B., Vulcan, P., Lane, J., 1994. Side impact crashes in Australia. In: Proceedings of the 14th International Technical Conference on Experimental Safety Vehicles.
- Gennarelli, T.A., Meaney, D.F., 1996. Mechanisms of primary head injury. In: Wilkins, R., Rengachary, S., (Eds.), *Neurosurgery*, 2nd ed., vol. 2. McGraw Hill, New York, pp. 2611–2621.
- Gennarelli, T., Pintar, F., Yoganandan, N., Beuse, N., Morgan, R., 2002. Head injuries to nearside occupants in lateral impacts: epidemiological and full-scale crash test analyses. In: Proceedings of the IRCOBI, Munich, Germany, pp. 223–233.

- Gloyns, P., Rattenbury, S., Weller, R., Lestina, D., 1994. Mechanisms and patterns of head injuries in fatal frontal and side impact crashes. In: Proceedings of the IRCOBI, Lyon, France.
- Got, C., Patel, A., Fayon, A., Tarriere, C., Walfisch, G., 1978. Results of experimental head impacts on cadavers: the various data obtained and their relations to some measured physical parameters. In: Proceedings of the 22nd Stapp Car Crash Conference, Ann Arbor, MI.
- Got, C., Guillon, F., Patel, A., Mack, P., Brun-Cassan, F., Fayon, A., Tarriere, C., Hureau, J., 1983. Morphological and biomechanical study of 126 human skulls used in experimental impacts, in relation with the observed injuries. In: Proceedings of the 27th Stapp Car Crash Conference, Bron, France.
- Gurdjian, E.S., Webster, J.E., 1946. Deformation of the skull in head injury studied by stresscoat technique. *Surg. Gyn. Obst.* 83, 219–233.
- Gurdjian, E.S., Webster, J.E., Lissner, H.R., 1947. The mechanism of production of linear skull fractures. *Surg. Gyn. Obst.* 85, 195–210.
- Gurdjian, E.S., Webster, J.E., Lissner, H.R., 1949. Studies on skull fracture with particular reference to engineering factors. *Am. J. Surg.*, 736–742.
- Gurdjian, E.S., Webster, J.E., Lissner, H.R., 1953. Observations on prediction of fracture site in head injury. *Radiology* 60, 226–235.
- Hodgson, V.R., 1967. Tolerance of the facial bones to impact. *Am. J. Anat.*, 120:113–122.
- Hodgson, V.R., Thomas, L.M., 1971. Breaking strength of the human skull vs. impact surface curvature. US Department of Transportation, HS-800-583, Springfield, VA.
- Hodgson, V.R., Thomas, L.M., 1972. Effect of long-duration impact on head. In: Proceedings of the 16th Stapp Car Crash Conference, Detroit, MI, pp. 292–295.
- Hodgson, V., Thomas, L., 1973. Breaking strength of the human skull vs impact surface curvature. DOT-HS-801-002.
- Hodgson, V.R., Thomas, L.M., Brinn, J., 1973. Concussion levels determined by HPR windshield impacts. In: Proceedings of the 17th Stapp Car Crash Conference, Oklahoma City, OK.
- Kleinberger, M., Yoganandan, N., Kumaresan, S., 1998. Biomechanical considerations for child occupant protection. In: Proceedings of the 42nd AAAM Conference, Charlottesville, VA, pp. 115–136.
- Lund, A.K., 2000. Recommended procedures for evaluating occupant injury risk from deploying side airbags. International Standard Organization, ISO-TR-1433.
- Maltese, M., Eppinger, R., Rhule, H., Donnelly, B., Pintar, F., Yoganandan, N., 2002. Response corridors of human surrogates in lateral impacts. *Stapp Car Crash J.* 46, 321–351.
- McElhaney, J.H., Stalnaker, R.L., Roberts, V.L., 1972. Biomechanical aspects of head injury. In: King, W., Mertz, H. (Eds.), *Human Impact Tolerance*. Plenum Press, New York, pp. 85–112.
- McElhaney, J.H., Roberts, V.L., Hilyard, J.F. (Eds.), 1976. *Handbook of Human Tolerance*. Japan Automobile Research Institute, Inc, Tokyo, Japan, p. 631.
- Messerer, O., 1880. *Über Elasticität und Festigkeit der Menschlichen Knochen*. Stuttgart, Germany.
- Mohan, O., Bowman, B.M., Snyder, R.G., Foust, D.R., 1979. A biomechanical analysis of head impact injuries to children. *J. Biomech. Eng.* 101, 250–259.
- Mosekilde, L., Mosekilde, L., 1986. Normal vertebral body size and compressive strength: relations to age and to vertebral and iliac trabecular bone compressive strength. *Bone* 7, 207–212.
- Nahum, A., Gatts, J.D., Gadd, C.W., Danforth, J., 1968. Impact tolerance of the skull and face. In: Proceedings of the 12th Stapp Car Crash Conference, Detroit, MI, p. 302.
- Nahum, A., Ward, C., Raasch, F., Adams, S., Schneider, D., 1980. Experimental studies of side impact to the human head. In: Proceedings of the 24th Stapp Car Crash Conference, Troy, MI.
- NHTSA, 1988. Department of Transportation Standard No. 218, Motorcycle helmets.
- NHTSA, 2002. Code of Federal Regulations, Title 49, Part 571. National Highway Traffic Safety Administration, Federal Motor Vehicle Safety Standards, Washington, DC.
- NHTSA, 2003. Available from <www.nhtsa.dot.gov>, Department of Transportation.
- NOCSAE, 1997. National Operating Committee on Standards for Athletic Equipment Doc. 002-96. Standard performance specification for newly manufactured football helmets.
- Ommaya, A.K., 1985. Biomechanics of head injury. In: Nahum, A.M., Melvin, J. (Eds.), *The Biomechanics of Trauma*. Appleton-Century-Crofts, Norwalk, CT, pp. 245–269.
- Ommaya, A., Yarnell, P., Hirsch, A., Harris, E., 1967. Scaling of experimental data on cerebral concussion in sub-human primates to concussion threshold in man. In: Proceedings of the 10th Stapp Car Crash Conference, pp. 73–80.
- Padgaonkar, A., Krieger, K., King, A., 1975. Measurement of angular acceleration of a rigid body using linear accelerometers. *J Appl. Mech.*, 552–556.
- Pintar, F.A., Yoganandan, N., Hines, M.H., Maltese, M.R., McFadden, J., Saul, R., Eppinger, R., Khaewpong, N., Kleinberger, M., 1997. Chestband analysis of human tolerance to side impact. In: Proceedings of the 41st Stapp Car Crash Conference, Lake Buena Vista, FL, pp. 63–74.
- Reynolds, H.M., Clauser, C.E., McConville, J., Chandler, R., Young, J.W., 1975. Mass distribution properties of the male cadaver. *Proceedings of the Society of Automotive Engineers*, 305–335.
- SAE, 1994. Human mechanical response characteristics.
- Sances Jr, A., Yoganandan, N., 1986. Human head injury tolerance. In: Sances Jr, A., Thomas, D.J., Ewing, C.L., Larson, S.J., Unterharnscheidt, F. (Eds.), *Mechanisms of Head and Spine Trauma*. Aloray, Goshen, NY, pp. 189–218.
- Sances, A., Myklebust, J.B., Larson, S.J., Cusick, J.F., Weber, R.C., Walsh, P.R., 1981. Bioengineering analysis of head and spine injuries. *CRC Crit. Rev. Bioeng.* 2, 1–79.
- Sances Jr, A., Thomas, D.J., Ewing, C.L., Larson, S.J., Unterharnscheidt, F. (Eds.), 1986. *Mechanisms of Head and Spine Trauma*. Aloray, Goshen, NY, p. 746.
- Schneider, D., Nahum, A., 1972. Impact studies of facial bones and skull. In: Proceedings of the 16th Stapp Car Crash Conference, Detroit, MI, pp. 186–203.
- Snell, 1995. Snell standard for protective headgear for use with bicycles.
- Snyder, R.G., Foust, D.R., Bowman, B.M., 1977. Study of impact tolerance through free fall investigations. IIHS, Washington, DC.
- Society of Automotive Engineers, 1980. Human tolerance to impact conditions as related to motor vehicle design-J885. SAE, Warrendale, PA.
- Stalnaker, R., Melvin, J., Nuscholtz, G., Alem, N., Benson, J., 1977. Head impact response. In: Proceedings of the 21st Stapp Car Crash Conference, New Orleans, LA, pp. 305–335.
- Tanner, J., 1962. *Growth at Adolescence*. Blackwell Scientific, Oxford.
- Tindall, G., Cooper, P., Barrow, D., 1996. In: *The Practice of Neurosurgery*. Williams and Wilkins, Baltimore, p. 2695.
- Van der vorst, M.J., Stuhmiller, J., Ho, K., Yoganandan, N., Pintar, F., 2003. Statistically based criterion for impact-induced skull fracture. *AAAM* 47, 487–507.
- Versace, J., 1971. A review of the severity index. In: Proceedings of the 15th Stapp Car Crash Conference, Coronado, CA, pp. 771–796.
- Voo, L., Kumaresan, S., Pintar, F.A., Yoganandan, N., Sances, A.J., 1996. Finite-element models of the human head. *Med. Biol. Eng. Comput.* 34, 375–381.
- Walker, L., Harris, E., Pontius, U., 1973. Mass, volume, center of mass, and mass moment of inertia of head and neck of human body. In: Proceedings of the 17th Stapp Car Crash Conference, Oklahoma City, OK, pp. 525–537.
- Williams, P.L., 1995. *Gray's Anatomy*. Churchill Livingstone, New York, p. 2092.

- Wood, J.L., 1971. Dynamic response of human cranial bone. *J. Biomech.* 4, 1–12.
- Yoganandan, N., Myklebust, J.B., Ray, G., Sances Jr, A., 1987. Mathematical and finite element analysis of spinal injuries. *CRC Rev. Biomed. Eng.* 15, 29–93.
- Yoganandan, N., Myklebust, J.B., Wilson, C.R., Cusick, J.F., Sances Jr, A., 1988. Functional biomechanics of the thoracolumbar vertebral cortex. *Clin. Biomech.* 3, 11–18.
- Yoganandan, N., Pintar, F.A., Sances, A.J., Harris, G., Chintapalli, K., Myklebust, J.B., Schmaltz, D., Reinartz, J., Kalbfleisch, J., Larson, S.J., 1989. Steering wheel induced facial trauma. *SAE Trans.* 97, 1104–1128.
- Yoganandan, N., Pintar, F.A., Sances Jr, A., 1991a. Biodynamics of steering wheel induced facial trauma. *J Safety Res.* 22, 179–190.
- Yoganandan, N., Sances Jr, A., Pintar, F.A., Larson, S., Hemmy, D., Maiman, D., Haughton, V., 1991b. Traumatic facial injuries with steering wheel loading. *J. Trauma* 31, 699–710.
- Yoganandan, N., Pintar, F.A., Reinartz, J., Sances Jr, A., 1993. Human facial tolerance to steering wheel impact: a biomechanical study. *J. Safety Res.* 24, 77–85.
- Yoganandan, N., Pintar, F.A., Sances, A.J., Walsh, P.R., Ewing, C.L., Thomas, D.L., Snyder, R.G., 1995. Biomechanics of skull fracture. *J. Neurotrauma* 12, 659–668.
- Yoganandan, N., Kumaresan, S., Voo, L., Pintar, F., 1996. Finite element applications in human cervical spine modeling. *Spine* 21, 1824–1834.
- Yoganandan, N., Pintar, F.A., Larson, S.J., Sances Jr, A. (Eds.), 1998. *Frontiers in Head and Neck Trauma: Clinical and Biomechanical*. IOS Press, The Netherlands, p. 743.
- Yoganandan, N., Kumaresan, S., Pintar, F., Gennarelli, T., 2000. Pediatric biomechanics. In: Nahum, A., Melvin, J. (Eds.), *Accidental Injury: Biomechanics and Prevention*. Springer-Verlag, New York, pp. 550–587.
- Yoganandan, N., Pintar, F., Maltese, M., Eppinger, R., Rhule, H., Donnelly, B., 2002. Biofidelity evaluation of recent side impact dummies. In: *Proceedings of the IRCOBI, Munich, Germany*, pp. 57–69.
- Youman, J., 1996. *Neurological surgery*. WB Saunders, Philadelphia. p. 3729.
- Zaouk, A., Eigen, A., Digges, K., 2001. Occupant injury patterns in side crashes. In: *Proceedings of the SAE World Congress, Detroit, MI*, 77–81.